Reactor and Technical Feasibility Aspects of a CO 2 Decomposition-Based Power Generation Cycle, Utilizing a High-Temperature Membrane Reactor

ARTICLE *in* INDUSTRIAL & ENGINEERING CHEMISTRY RESEARCH · JUNE 2003

Impact Factor: 2.59 · DOI: 10.1021/ie020980r

6 AUTHORS, INCLUDING:

Yiqun Fan
Nanjing Tech University
74 PUBLICATIONS **913** CITATIONS

SEE PROFILE

Reactor and Technical Feasibility Aspects of a CO_2 Decomposition-Based Power Generation Cycle, Utilizing a High-Temperature Membrane Reactor

Yiqun Fan,[†] Jyh-yih Ren,[‡] William Onstot,[†] Jay Pasale,[†] Theodore T. Tsotsis,*[,†] and Fokion N. Egolfopoulos[‡]

Departments of Chemical Engineering and of Aerospace and Mechanical Engineering, University of Southern California, Los Angeles, California 90089

The technical feasibility of separating and decomposing CO_2 in the context of a novel energy generation cycle during the operation of a glass furnace was investigated. The concept envisions CO_2 decomposition to take place in a membrane reactor utilizing high-temperature solid-oxide membranes with the aid of oxygen chemical pumping. The glass furnace environment is well suited for such an application because it provides the high-temperature conditions needed for the operation of these membranes. As part of this effort, solid-oxide membranes were prepared and their oxygen permeation was measured in a membrane reactor system. The O_2 permeabilities in the presence of a reactive sweep were significantly higher than the corresponding permeabilities measured in the presence of He as a sweep gas. These membranes were utilized for CO_2 decomposition in a membrane reactor. Conversions significantly higher than the expected thermodynamic equilibrium values were attained. Engineering calculations of the overall glass furnace efficiency were also carried out, and the conditions for optimal performance were determined. The effects of the application of this novel cycle on glass furnace operation in terms of combustion stability (quantified by the extinction strain rates of the relevant combustion mixtures) and pollutant (NO_x) emissions were also determined. Generally, improvements in combustion intensity and stability can be achieved but at a cost of increased NO_x emissions and vice versa. A range of conditions also exists for which the cycle allows for effective waste heat utilization without undue impact on pollutant emissions.

Introduction

One novel concept currently investigated by our group[1] is an energy generation cycle incorporating recuperation of waste heat through CO_2 decomposition

$$2CO_2 \leftrightarrow 2CO + O_2 \qquad \text{(R1)}$$

in a membrane reactor with the aid of high-temperature solid-oxide membranes. A first step in this concept is the separation of CO_2 from the flue gas, followed by reaction of the separated gas in a membrane reactor. CO_2 decomposition into CO and O_2 is a highly endothermic reaction (552 kJ/mol) that lends itself easily to CO_2 emissions reduction as part of an energy generation cycle involving waste heat recuperation. The concept is an equally (if not more) effective means for waste heat recouping and utilization than catalytic reforming based technologies. Waste heat recuperation significantly improves the power/energy production efficiency.[2] This, in turn, minimizes the use of fossil fuel resources and the release into the atmosphere of additional amounts of CO_2. The CO_2 decomposition technology has, furthermore, the additional benefit that it produces pure O_2. This may significantly impact the economics of energy generation in select industries (e.g., the glass industry, waste incineration, etc.). It may also result in additional substantial reductions in CO_2 emissions because the production of oxygen is currently an energy-intensive operation.

Though innovative for energy applications, CO_2 decomposition carried out in a membrane reactor is not an untried concept.[3,4] For example, the use of solid-oxide electrochemical reactors for CO_2 decomposition has been studied for a number of years in the space program for manned missions to Mars[5] and has been proven technically feasible. Adapting such technology for the energy generation marketplace still remains a challenge, however. The focus in our own research is on the use of conventional membrane reactors, which eliminate the need for using an external electronic circuit. Prior similar efforts[3,4] were successful in validating the concept. Nigara and Cales,[3] for example, utilized a calcia-stabilized zirconia membrane reactor to study the thermal decomposition of carbon dioxide in the context of thermal energy storage. At 1954 K, the conversion of carbon dioxide in the membrane reactor reached 21.5% by using carbon monoxide as a sweep gas; the corresponding thermodynamic equilibrium conversion at the same temperature is only 1.2%. Itoh et al.[4] studied the thermal decomposition of CO_2 with a yittria-stabilized zirconia (YSZ) membrane reactor system. The experiments were carried out in the temperature range of 1584−1782 K, and argon was used as a sweep gas. Because argon cannot supply a low enough oxygen partial pressure, the highest CO_2 conversion reported in the experiments of Itoh et al.[4] was about 0.6%, still above the expected thermodynamic equilibrium conver-

* To whom correspondence should be addressed. Tel.: 213 740 2069. Fax: 213 740 8953. E-mail: Tsotsis@usc.edu.
[†] Department of Chemical Engineering.
[‡] Department of Aerospace and Mechanical Engineering.

10.1021/ie020980r CCC: $25.00
Published on Web 05/07/2003

sion. The reactor temperatures utilized in both of these investigations (~1600 K or higher) are beyond the temperature range where waste heat utilization is efficient and/or possible. The need for high temperatures is because the materials utilized in these two studies are poor electronic conductors. The focus in our research is on using materials that have both good electronic and ionic conductivities, thus eliminating the need for very high temperatures or for maintaining an external electronic circuit.

The emphasis in our previous paper[1] was on combustion issues related to the integrated CO_2 capture energy generation cycle. While the combustion characteristics of natural gas (which consists mostly of CH_4) have been extensively studied over the years, the knowledge regarding the combustion of fuel mixtures containing CH_4, CO, and CO_2 is quite limited.[6,7] In the implementation of the cycle, all three components are present in significant amounts in the fuel mix, and each component affects the overall combustion process. Laminar flame speeds, extinction strain rates, and NO_x emissions for such flames were measured and presented.[1] Numerical simulations of the same flames were also described. Good agreements have been found between experiments and simulations.

In this paper, additional important aspects of the overall process are described. In our work, the thermal decomposition of CO_2 is studied in a membrane reactor with dense $SrCo_{0.5}FeO_3$ membranes. Similar materials were previously studied by other investigators[8−11] and were shown to have good stability in reducing reactive environments. In this paper, we describe their preparation, characterization, and use in a membrane reactor for the decomposition of CO_2. Another aspect of the ongoing effort relates to the performance and overall efficiency of the proposed integrated process; in this paper, the process design characteristics are analyzed for the case of a glass furnace. The fraction of CO_2 that is recycled and the membrane reactor operating temperature are key operating parameters that determine the overall performance and cycle efficiency, and their effects are analyzed and presented. The good agreements that have been found between experiments and simulations[1] have provided confidence for using detailed numerical simulations to probe further the complex characteristics of this energy generation cycle. In this paper, we probe and present further aspects of flame stability and pollutant emissions. We analyze the requirements for maintaining good combustion stability for the wide variety of fuel compositions that may be employed in the cycle. NO_x emissions remain a focus, particularly in relationship to the overall cycle efficiency, because it is undesirable to have the CO_2 remediation efforts result in the increase of the emissions of other key pollutants.

CO_2 is a significant contributor to the "greenhouse effect",[12,13] and the furnace/boiler industry is one of its key producers. Direct CO_2 decomposition using waste heat is potentially attractive as a future efficient and compact CO_2 emissions reduction technology that is easy to retrofit within existing systems. Though promising, the proposed technology still faces important hurdles, key among which is the long-term performance of these materials in the energy generation environment; this remains an ongoing focus of our research.

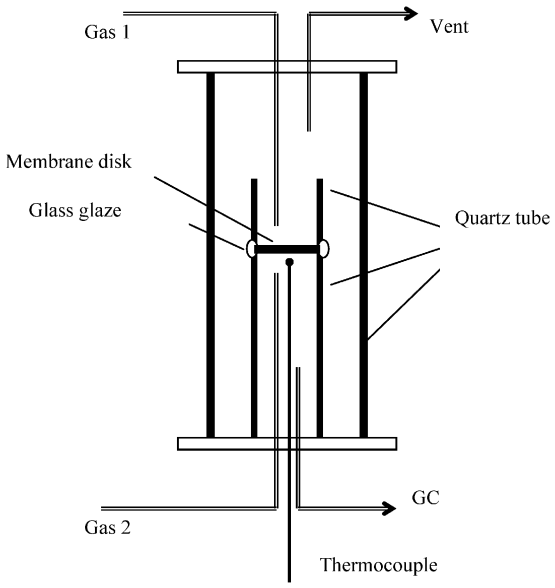

Figure 1. Schematic of the experimental apparatus.

Experimental Approach

The membranes utilized in this work were made from a ceramic $SrCo_{0.5}FeO_3$ powder prepared by the solid-state reaction route.[8] $SrCO_3$ (99% pure, from Aldrich), Fe_2O_3 (99.945% pure, from Johnson Matthey), and $Co(NO_3)_2 \cdot 6H_2O$ (99% pure, from Mallinckrodt Baker Inc.) were precisely weighed, so that after the solid-state reaction they would create a compound with a molar composition of that of $SrCo_{0.5}FeO_x$. They were then mixed by ball-milling with zirconia balls for 20 h. The mixtures were calcined at 1123 K for 16 h in air. The calcined powder mixture was ground in a mortar and pestle and was again ball-milled. The powder was then mixed in a mortar, with a poly(vinyl alcohol) solution added as a binder, and was pressed isostatically at 150 MPa for 1 min to form a disk (33 mm diameter and 2 mm thickness). After drying, the green sample was placed in an alumina sample holder and inserted in a programmable high-temperature furnace. The temperature of the sample was raised at 1 K/min, until the temperature reached 773 K; after that the temperature was raised again at a rate of 2 K/min until a preselected temperature was reached. The disk is calcined at this temperature, typically for 2−5 h. The crystal structure of the resulting $SrCo_{0.5}FeO_3$ membrane disk was determined by X-ray powder diffractometry (XRD) in a Rikago diffractometer with Cu Kα radiation.

The experimental membrane reactor apparatus is shown in Figure 1. For the oxygen permeation measurements, air was fed to the top chamber (gas 1) and helium or a mixture of helium and methane was fed to the bottom chamber (gas 2). The content of oxygen or carbon dioxide was determined with a Varian 3400 gas chromatograph using a carbon molecular sieve packed column and helium as the carrier gas. For the CO_2 decomposition reaction experiment, CO_2 diluted with helium was fed to the bottom chamber (gas 2) and methane mixed with argon was fed to the top membrane reactor chamber (gas 1). CO_2 decomposed to oxygen and carbon monoxide. Oxygen permeates through the solid-oxide membrane; carbon monoxide and the unreacted CO_2 remain in the reactor chamber and are analyzed by gas chromatography.

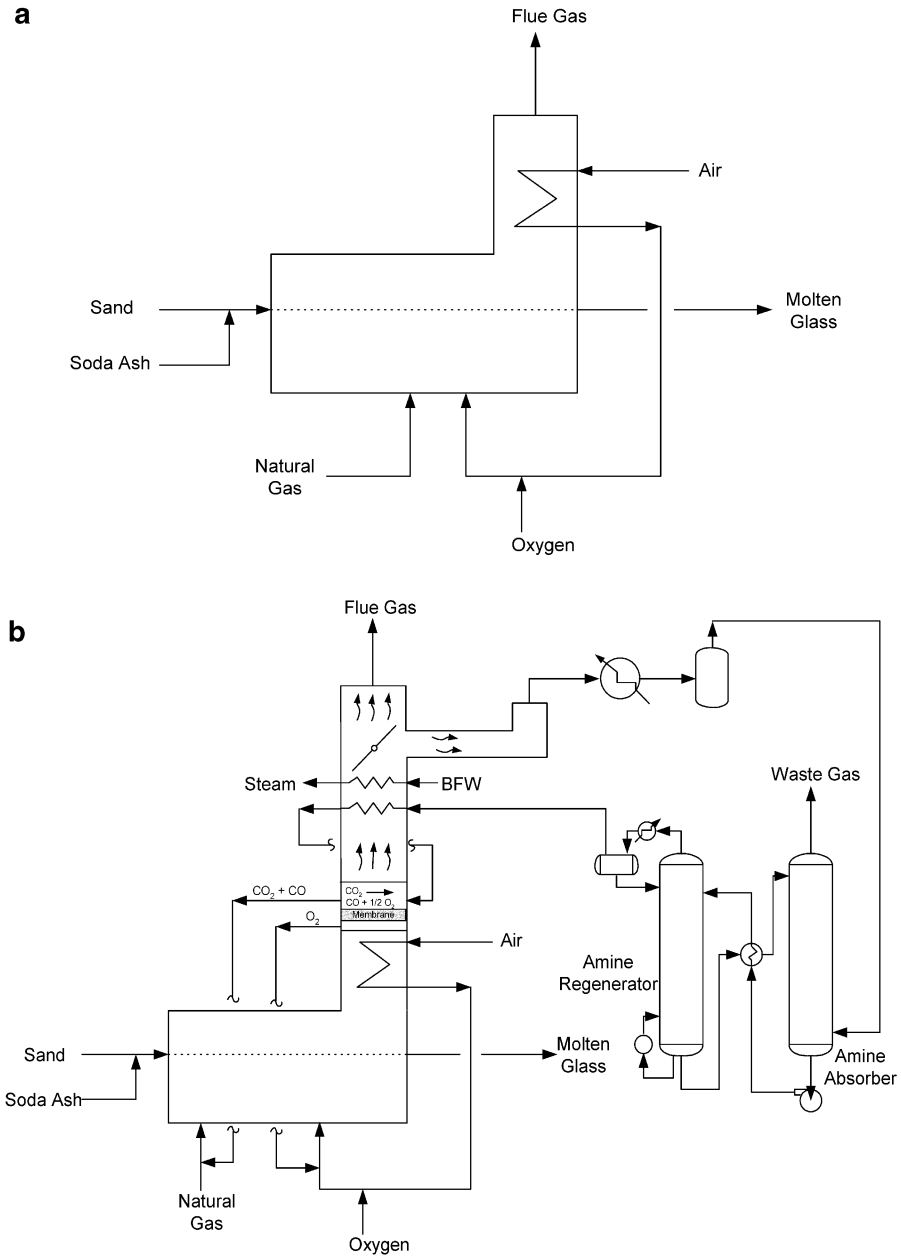

Figure 2. (a) Schematic of a conventional glass furnace. (b) Membrane-equipped glass furnace.

Numerical Approach

The numerical simulations for the determination of the extinction strain rates and NO_x concentration of an atmospheric CH_4/air flame in the presence of binary CO/CO_2 mixtures that would result from the CO_2 decomposition process were conducted by using the one-dimensional stagnation-flow code[14] solving for the steady-state mass, momentum, energy, and species conservation equations along the stagnation streamline in a finite domain. In this code, radiative transfer from CH_4, H_2O, CO_2, and CO was included.[15,16] The code was linked to the Chemkin-II[17] and Transport[18] subroutine libraries. The GRI 3.0 mechanism[19] was used for the description of the C_1- and C_2-hydrocarbon oxidation and NO_x kinetics.

Results and Discussion

Design Aspects of the Overall Integrated Process. In this paper, we examine the application of the waste heat recuperative cycle based on CO_2 decomposition in the context of high-temperature processes that utilize oxygen. Prime examples of such a process are the continuous recuperative furnaces employed in the glass industry. In these furnaces, sand (SiO_2) and soda ash (Na_2CO_3) are melted and fused at high temperature (in excess of 1810 K) in a continuous furnace. To attain the high temperatures required, these furnaces are fired with natural gas and air supplemented with oxygen (they may also be assisted with electrical heating). While some of flue gas from the furnace is used to preheat the combustion air, most of the sensible heat contained in the flue gas is lost to the atmosphere. This conventional arrangement is shown schematically in Figure 2a. Because large quantities of steam are generally not required in the glass-making operation, there is little incentive for additional heat recovery from the flue gas. As a result, the flue gas typically exits the furnace at temperatures of 1920−2200 K, which translates into an overall furnace efficiency of about 30%.[20]

Here, the furnace efficiency is defined as

$$\% \text{ efficiency} = (\text{heat absorbed by the process} + \text{heat absorbed by air preheat})/\text{heat of combustion (LHV)}$$

where LHV = lower heating value of fuel.

This low overall efficiency may be potentially improved and a reduction in the fuel and oxygen requirements may be obtained by coupling the furnace operation with that of a membrane reactor equipped with an oxygen-permeable membrane, and utilizing the waste heat in the flue gas to drive the dissociation of CO_2 into CO and O_2. One configuration for such a process is shown schematically in Figure 2b. The level of technical detail shown in Figure 2b is appropriate for the design calculations to be presented here. In practice, materials and reactor performance issues are likely to dictate the technical aspects of integration of the reactor system within the furnace environment (e.g., placing the reactor in a reductive zone in the furnace).

In our design calculations of the overall integrated system as a first step, the flue gas from the furnace is cooled, first by heat exchange with the membrane reactor and the CO_2 reheat coil and then by the steam generation coil and an external heat exchanger. The cooled flue gas then enters the amine absorber, which recovers the CO_2 from the flue gas, with the waste gas exiting in the absorber overhead. The rich amine is pumped to the amine regenerator, where the CO_2 is recovered. This arrangement differs from a traditional amine system because the absorption takes place at low pressure while the amine regeneration takes place at a higher pressure. This arrangement, however, does permit the CO_2 to be recovered at a higher pressure for use in the membrane reactor section of the process. The steam required for the amine regenerator is generated in the convection section of the furnace. From the amine regenerator, the CO_2 is preheated by the flue gas and fed to the membrane section of the process. Here, the hot flue gas is used to drive the dissociation of CO_2 to CO and O_2. The oxygen is recovered on the other side of the membrane. The raffinate CO/CO_2 is returned to the furnace as fuel, while the oxygen is utilized with the combustion air.

The flue gas heat recovery for the conventional glass furnace and the furnace equipped with the membrane reactor are shown in parts a and b of Figure 3. The basis for these heat curves is methane fuel gas, with oxidant comprised of 50% air and 50% oxygen and containing 20% more oxygen than is required for the stoichiometric combustion of the fuel. The process load (sand and soda ash) is assumed to melt and fuse at 1810 K, with the flue gas leaving the furnace at 2200 K (i.e., a 390 K temperature approach). The efficiency for this example is 32.9%. The additional heat recovery accomplished by the membrane-equipped process is shown in Figure 3b. In this example, the membrane reactor is assumed to operate isothermally at 1260 K with 90% conversion. Half of the CO_2 contained in the furnace flue gas is absorbed and used as a membrane reactor feed. Because the CO/CO_2 from the furnace is returned as fuel to the furnace firebox, the adiabatic flame temperature in the furnace increases from 2600 K for the conventional glass furnace to 2880 K for the membrane-equipped furnace. When the same 1810 K process temperature and the same process-to-flue gas approach temperature of 390 K are maintained, the efficiency of the process is increased to 65.7%, twice that of the conventional glass furnace. Thus, fuel and purchased oxygen consumption are reduced by half. For the membrane-equipped furnace, the efficiency is defined as

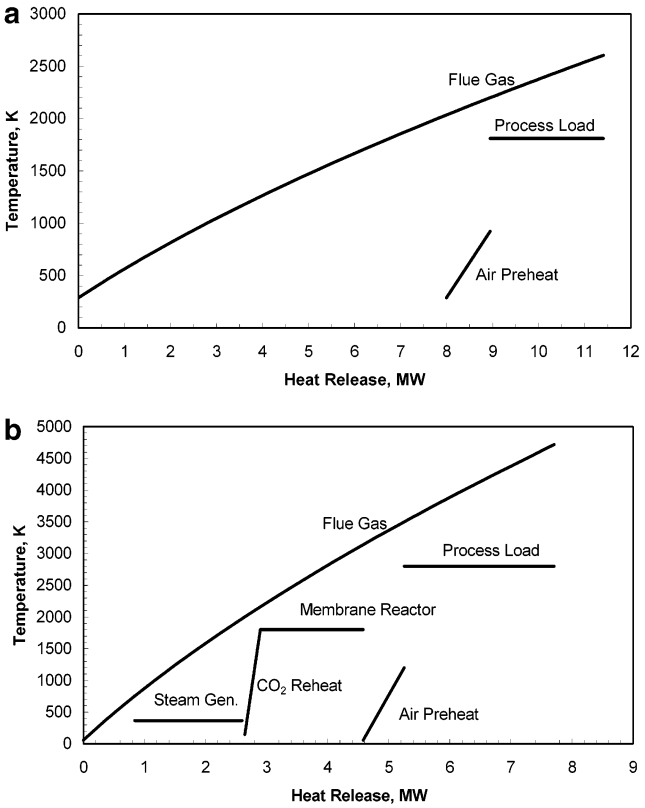

Figure 3. (a) Flue gas heat curve for a conventional glass furnace. (b) Flue gas heat curve for a glass furnace coupled with the CO_2 decomposition process.

$$\% \text{ efficiency} = (\text{heat absorbed by the process} + \text{heat absorbed by air preheat} + \text{heat absorbed by the membrane reactor} + \text{CO}_2 \text{ reheat})/\text{heat of combustion (LHV)}$$

Note that no credit for heat used to generate steam for the amine regenerator is taken because this energy does not directly translate into a reduction in fuel fired. This example illustrates the fundamental benefit of the process: the additional heat recovery accomplished in the membrane reactor is liberated at a temperature that is useable by the process load. Because conventional glass-making facilities have little use for utilities such as steam, the only option for recovering heat from the flue gas is air preheat. With the CO_2 recovery process, heat that would otherwise be wasted in the flue gas is upgraded for use to either melt and fuse additional glass or to reduce the fuel and oxygen requirements for a given process load.

The effects of various operating parameters on the furnace efficiency are summarized in Figure 4. This figure uses the same calculation basis as the example above: a process temperature of 1810 K and a 390 K process-to-flue gas temperature approach. The recycle

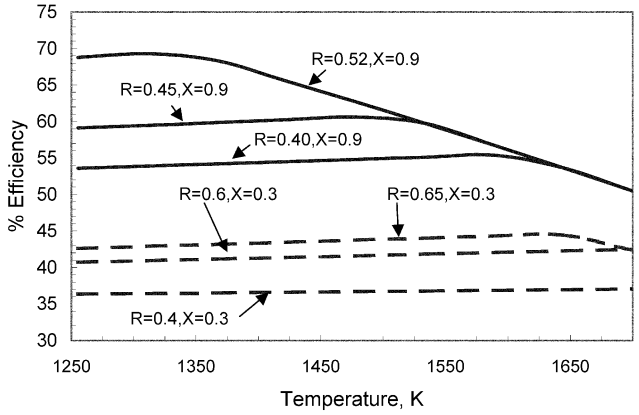

Figure 4. Furnace efficiency as a function of the reactor temperature for various recycle ratios, *R*, and 30% and 90% reactor conversions, *X*.

ratio *R* and the membrane reactor conversion *X* are defined as

$$R = \frac{\text{moles of } CO_2 \text{ absorbed in the absorber}}{\text{total moles of } CO_2 \text{ in the flue gas}}$$

$$X = \frac{\text{moles of } CO_2 \text{ dissociated in the reactor}}{\text{moles of } CO_2 \text{ fed to the reactor}}$$

The amine absorber/regenerator system is assumed to use a 20 wt % monoethanolamine solution with an amine loading ratio of 0.35 mol of CO_2/mol of amine. As shown in Figure 4, for a given reactor conversion, the overall efficiency increases modestly with increasing reactor temperature to some maximum and then begins to fall rapidly. The initial modest increase in the furnace efficiency with increasing reactor temperature is the result of the additional heat recovery required to preheat the CO_2 stream to the reactor temperature. However, a maximum in the furnace efficiency is reached, which represents the maximum possible flue gas heat recovery attained at this particular reactor temperature. At higher reactor temperatures, there is insufficient heat in the flue gas to react all of the CO_2 fed to the reactor; as a result, additional fuel must be fired, resulting in a decrease in the overall furnace efficiency. Note that the CO_2 recycle ratio is limited to $R = 0.52$ for a membrane reactor with 90% conversion; at higher recycle ratios, not enough heat is available in the flue gas to generate the required steam for the amine regenerator reboiler. At lower reactor conversions, less heat is required for the membrane reactor, and consequently, more heat is available for steam generation and higher recycle ratios may be utilized. For the 30% case, the maximum recycle ratio is $R = 0.65$. From Figure 4, the importance of reactor conversion is immediately apparent. While to some extent it is possible to compensate for low reactor conversion by increasing the CO_2 recycle ratio, the availability of heat for steam generation ultimately limits this tradeoff. Figure 5 summarizes the effect on the furnace efficiency of the recycle ratio and reactor conversion. It is clear from these simulations that reactor conversion has a very significant effect on the furnace efficiency particularly under the high CO_2 recycle ratios. The key, therefore, to the success of the proposed process is the development of membrane reactors that attain the highest possible conversion for the lowest allowable operating temperature.

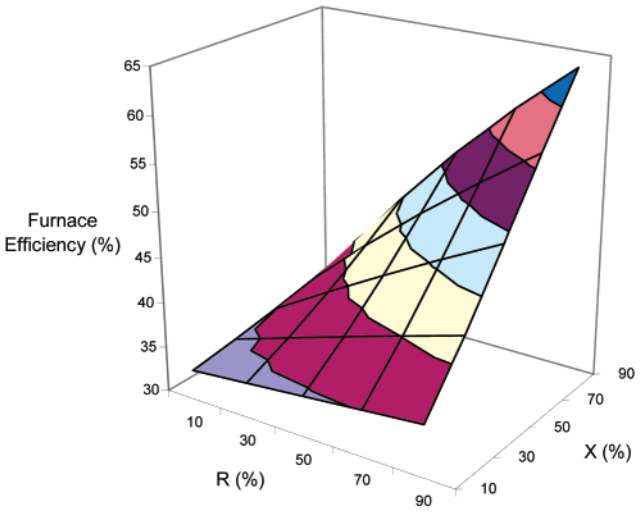

Figure 5. Calculated furnace efficiency as a function of the CO_2 recycle ratio in the fuel, *R*, and reactor conversion, *X*.

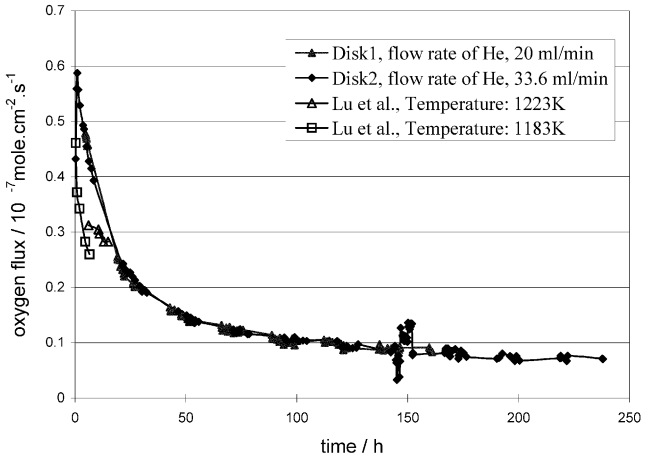

Figure 6. Oxygen flux of two $SrCo_{0.5}FeO_3$ membrane disks (temperature, 1173 K). Shown also on the figure are data by Lu et al.[10]

Membrane Reactor Experiments. The XRD pattern of the $SrCo_{0.5}FeO_3$ membranes used in our experiments has been presented elsewhere.[21] It is similar to the one reported by Balachandran et al.,[8,9] which proves that the materials prepared by our group are the same (in terms of their XRD signature) with the materials reported in the literature. Figure 6 depicts the O_2 permeation fluxes of two different $SrCo_{0.5}FeO_3$ membrane disks prepared by our group, measured using He as a sweep gas and for the same temperature of 1173 K. Oxygen fluxes at different temperatures for one of these membranes (taken during the period of 142−152 h in the experiments of Figure 6) are shown in Figure 7. The oxygen flux values shown in Figures 6 and 7 are similar to those reported by Lu et al.[10] (for comparison, some of these data are also shown in Figure 6). It should be noted from Figure 6 that we are able to prepare membranes with highly reproducible properties when measured under inert conditions. To test the oxygen permeation under reactive conditions, experiments have also been carried out in which He was replaced with a reactive sweep consisting of a mixture of CH_4 in He. The oxygen fluxes of a $SrCo_{0.5}FeO_3$ membrane disk under reactive conditions are shown in Figure 8. The O_2 fluxes in the presence of the reactive sweep are significantly higher than the fluxes measured in the

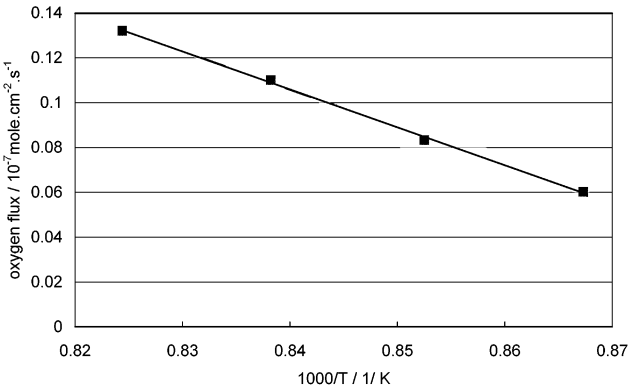

Figure 7. Oxygen flux at different temperatures.

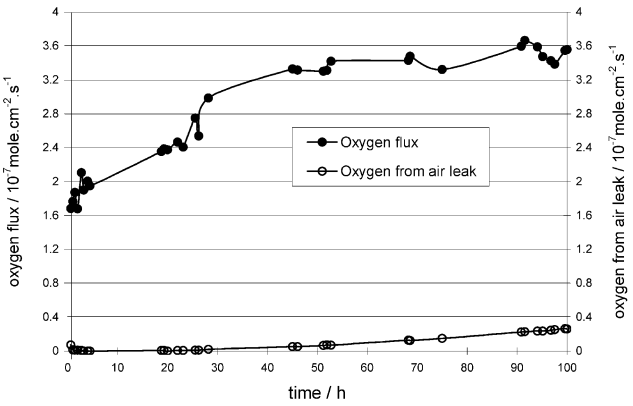

Figure 8. Oxygen flux of a $SrCo_{0.5}FeO_3$ membrane disk with a reactive sweep (air flow, 108 mL/min; sweep gas consists of helium at 10 mL/min + methane at 10 mL/min; temperature, 1173 K).

presence of the He sweep gas (their values are similar to those reported by Balachandran et al.[8]). Interesting to note is also that the disks behave qualitatively differently under inert and reactive conditions. While under inert conditions the flux declines significantly for a period of hours before it levels off, the opposite is true for the experiments under reactive conditions. Shown also in Figure 8 is the oxygen flux due to air leaking either through pinholes and microcracks in the membrane or through the glass seals. This leak flux is calculated on the basis of the amount of nitrogen that one observes in the sweep (permeate) chamber. For the data shown in Figure 8, the oxygen flux due to the air leak corresponds at most to less than 7% of the oxygen flux through the membrane. With the time on stream increasing, however, the air leak increases, indicative potentially of additional pinholes and microcracks developing through the membrane and/or the seals. For the membrane of Figure 8, for example, after 10 days continuously on stream the oxygen flux due to the air leak rose to about 20% of the flux through the membrane itself. Improving the thermal and mechanical stability of membrane materials and seals in these types of reactive environments remains a key challenge of our ongoing research activities.

Experiments with the CO_2 decomposition reaction were also carried out in the membrane reactor using $SrCo_{0.5}FeO_3$ membranes. The flow in the reactor chamber consists of a mixture of CO_2 in He, while the permeate side is swept with a reactive mixture consisting of a mixture of methane in argon, which acts as an inert and a leak tracer. Figure 9 depicts the behavior observed with one of these membranes. The reactor conversion starts typically low and then increases to

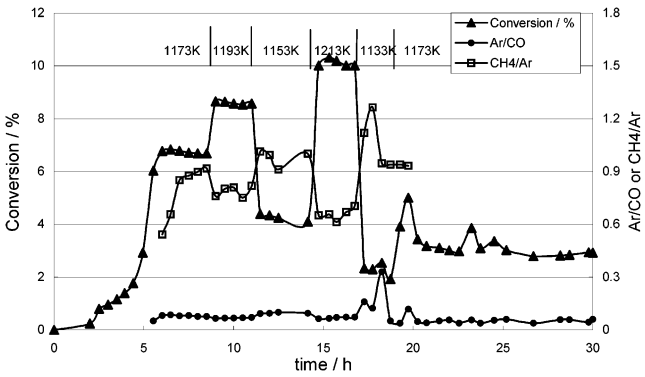

Figure 9. Effect of the temperature on CO_2 decomposition conversion in a ceramic membrane reactor (sweep gas consists of Ar at 30 mL/min + CH_4 at 24 mL/min; reactor feed consists of CO_2 at 12 mL/min + He at 48 mL/min; temperature, 1173 K).

higher values (for the particular membrane disk of Figure 9, the CO_2 decomposition reaction conversion reaches slightly above 6.7% at the temperature of 1173 K). After a few hours at this temperature for the experiments of Figure 9, the temperature was changed to 1193 K and the reactor conversion was noted for a few more hours. After that, three more temperatures (1153, 1213, and 1133 K) were studied. Upon return of the disk to the original temperature of 1173 K, the attained conversion is lower than the one noted earlier in the experiments, indicating a gradual change in the membrane properties. That the membrane changes as a result of exposure to the reactive gases is also manifested by the fact that after a certain number of hours on stream significant pinholes and cracks develop, which make the operation of the membrane reactor difficult. The causes for this membrane deterioration are currently under investigation by our group. As noted above, leaks for these high-temperature membrane reactor experiments are always a concern; infiltration of the reactive sweep (CH_4) into the reactor chamber either through pinholes and microcracks in the membrane disk itself or through the glass seals may potentially lead to falsification of the reactor conversion data. In the experiments in Figure 9 (and in all other experiments), the presence of Ar (used as a diluent on the sweep chamber) and CH_4 were monitored. The molar ratios of Ar to CO and CH_4 to Ar in the reactor chamber are also indicated in Figure 9. For the most part, the Ar/CO ratio stays below 0.1. In addition, while there is some variability in the CH_4/Ar ratio, it does not stray far away from the sweep feed molar ratio value of 0.8; this is indicative of the fact that the CO that is measured results from the CO_2 decomposition reaction rather from direct interaction of CH_4 with CO_2 or the membrane surface. Parts a and b of Figure 10 depict the effect of changing the CO_2 concentration in the feed on reactor conversion and flux for a different disk (for this particular disk, the reactor conversions and oxygen flux attained are slightly lower than the corresponding values for the disk of Figure 9). Interestingly, the conversion decreases as the CO_2 feed concentration increases. The oxygen flux, though, while it first increases (Figure 10b), levels off to a constant value. In Figure 10a, again one observes a gradual decline in the reactor conversion.

Though the reported experimental conversion values are rather low, one must note that they are orders of magnitude higher than what would be attained in a conventional reactor. Typical simulated membrane re-

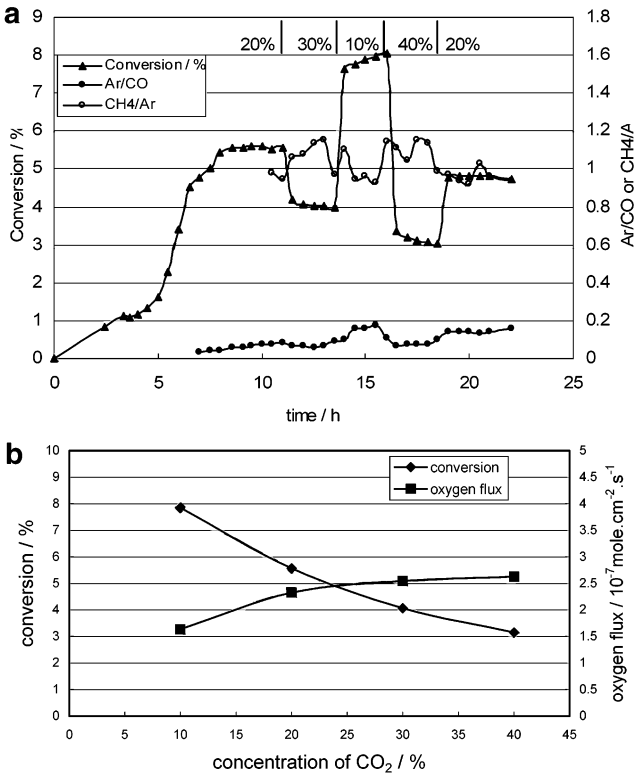

Figure 10. (a) CO_2 decomposition conversion as a function of time for different CO_2 mole fractions in the feed (sweep gas consists of Ar at 30 mL/min + CH_4 at 24 mL/min; reactant gas consists of CO_2 + He at 60 mL/min; temperature, 1173 K). (b) Influence of the CO_2 feed concentration on the CO_2 decomposition conversion (sweep gas consists of Ar at 30 mL/min + CH_4 at 24 mL/min; reactant gas consists of CO_2 + He at 60 mL/min; temperature, 1173 K).

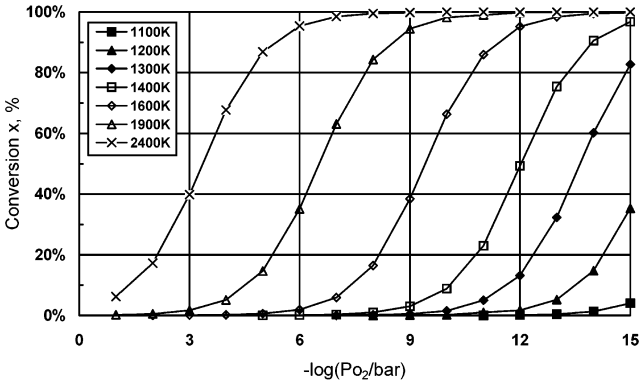

Figure 11. Simulated membrane reactor conversions as a function of oxygen partial pressure in the permeate chamber and reactor temperature.

actor conversions attained (based on the assumption that the membrane-side oxygen partial pressure equilibrates with that of the permeate side) are shown in Figure 11. The required permeate-side oxygen partial pressures needed to attain conversions similar to those reported here can be easily attained in reductive combustion environments, as the results shown in Figure 12 indicate. On the other hand, the experimental behavior shown in Figures 9 and 10 makes it clear that surface processes are likely to be intimately involved in the observed reactor behavior. Currently, experiments are under way with the bottom reactor chamber operating in a batchwise manner trying to shed additional light on the membrane reactor behavior.

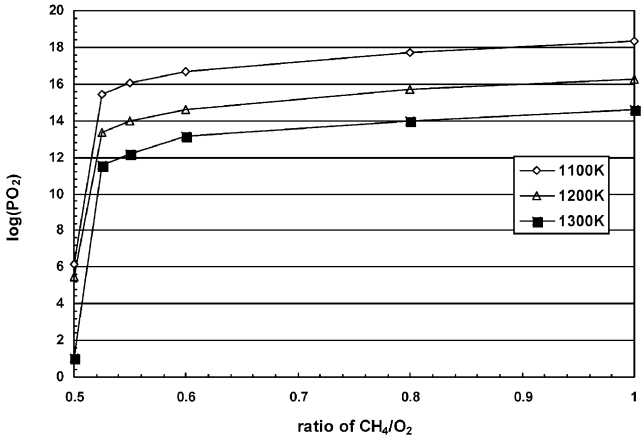

Figure 12. Simulated oxygen partial pressure in the permeate chamber as a function of the feed CH_4/permeated O_2 ratio and temperature.

Combustion Stability and Pollutant Emission Aspects. It is important for the potential application of the proposed process that the integration of the reactor into the furnace does not negatively impact its operation in terms of combustion stability and pollutant emissions. To quantitatively assess these characteristics, one must, of course, have detailed knowledge of the specific glass furnace configuration. One can develop, however, some generic guidelines by considering model combustor configurations.[1] A good measure of stability (blow-off limits) for a burner that is processing a given combustible mixture can be provided by the extinction strain rate (K_{ext}), which is a fundamental flame property for the combustible mixture. To measure the extinction strain rate (K_{ext}), one utilizes the stagnation-flow experimental configuration, in which planar flames are established between a nozzle and a plate that acts as the stagnation plane. Velocity profiles are measured along the centerline. Typically, the velocity profile has a near-zero gradient at the nozzle exit and gradually develops an increasing slope, which reaches its maximum just before the minimum velocity point, where heating starts. This maximum velocity gradient is defined as the imposed strain rate, K. In the stagnation-flow experimental configuration, increasing the nozzle exit velocity increases K and the flame is pushed toward the stagnation plane. A critical value of K exists, defined as the extinction strain rate K_{ext}, where for a further increase in the exit velocity the flame is extinguished. Higher values of K_{ext} typically signify stronger and more stably burning flames.[1,22] Figure 13, for example, depicts the simulated extinction strain rates for a number of combustion mixtures directly related to the furnace configuration in Figure 2b. For all of these flames, the equivalence ratio, i.e., ϕ_{total}, defined as $[(Y_{CO} + Y_{CH_4})/Y_{O_2}]/[(Y_{CO} + Y_{CH_4})/Y_{O_2}]_{stoich}$ (where Y_i is the mole fraction of species i), is maintained constant and equal to 0.7 by adjusting the flow of oxidant (air) into the furnace. In Figure 13(top), the simulated K_{ext} for CO_2/CO/CH_4/air flames for constant $\phi_{total} = 0.7$ is shown. For lower levels of conversion and for a given reactor conversion, K_{ext} decreases as the cumulative CO_2/CO fraction in the feed to the combustor increases. As the level of conversion increases, however, the decrease becomes more gradual and eventually K_{ext} increases with the cumulative CO_2/CO fraction. The behavior shown here can be explained on the basis of the effect that CO_2 and CO individually have on K_{ext}. For low reactor conversions, mostly CO_2

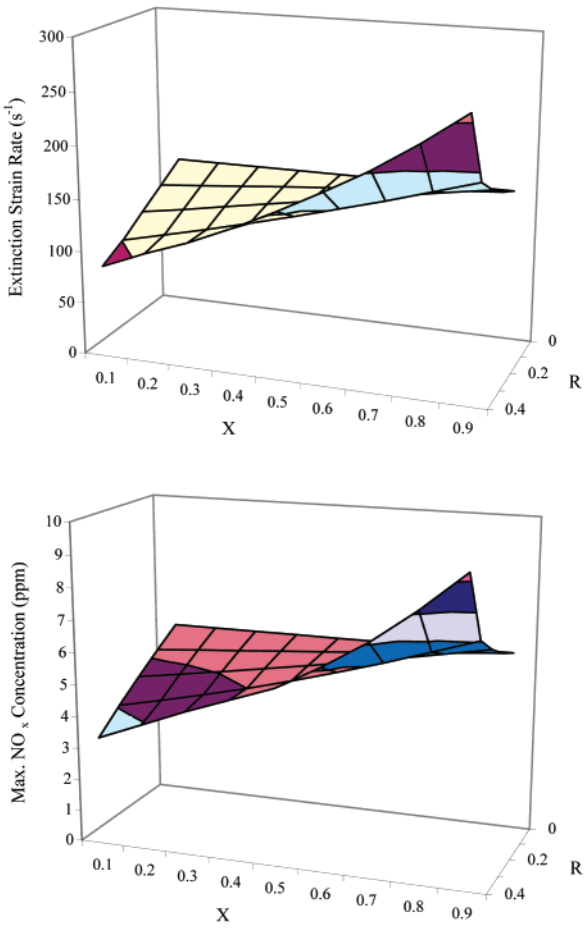

Figure 13. Calculated (top) K_{ext} and (bottom) maximum NO_x concentration as a function of the CO_2 recycle ratio R and reactor conversion X ($\phi_{total} = 0.7$).

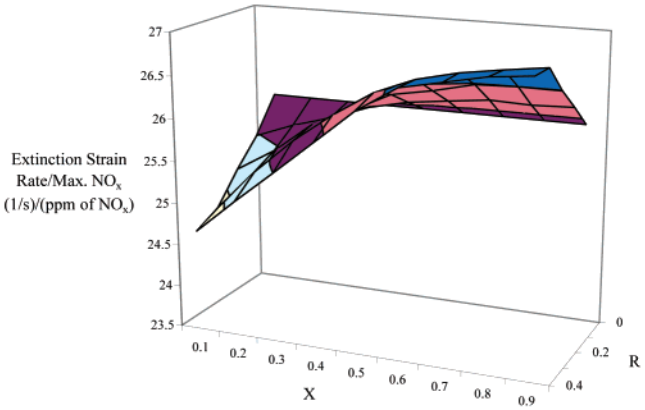

Figure 14. Calculated ratio of extinction strain rate/maximum NO_x concentration as a function of the CO_2 recycle ratio R and reactor conversion X ($\phi_{total} = 0.7$).

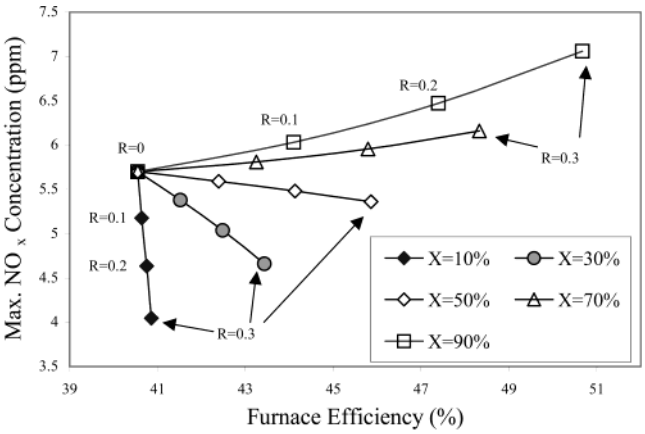

Figure 15. Calculated maximum NO_x concentration as a function of the furnace efficiency, CO_2 recycle ratio R, and reactor conversion X ($\phi_{total} = 0.7$).

enters the combustor and has a negative impact on K_{ext}. For higher reactor conversions, more CO is produced and enters the combustor, which has a positive effect on flame stability characteristics by enhancing the burning rate of such fuel-lean flames.

Of concern also are the pollutant emission characteristics (for gas furnaces, this mostly means NO_x) for the integrated process. Figure 13(bottom) depicts the maximum NO_x concentration, $C_{NO_{x,max}}$, in ppm observed for combustion mixtures relevant to the process configuration shown in Figure 2b. The $C_{NO_{x,max}}$ values shown in this figure were produced by simulations from the combustion of these mixtures in a model stagnation-flow configuration (as noted above, in our prior publication,[1] our simulations have been experimentally validated). Note that in Figure 13(bottom), for lower levels of conversion, $C_{NO_{x,max}}$ decreases with the cumulative CO_2/CO fraction. As the level of conversion increases, the decrease is no longer that profound. For higher levels of conversion, C_{NO_x} increases with the cumulative CO_2/CO fraction. This behavior can be explained by considering the individual effects that CO and CO_2 have on NO_x emissions. Increasing the CO mole fraction results in higher NO_x production, given that the CO addition increases the flame temperature. On the other hand, adding CO_2 tends to decrease the flame temperature and, consequently, the NO_x production, given that CO_2 acts mostly as a diluent. The observed response of $C_{NO_{x,max}}$ with the reactor conversion and the cumulative CO_2/CO fraction is similar to the one observed for K_{ext}, which is anticipated given that both NO_x (thermal NO_x) and extinction are high-temperature phenomena.

A key index for judging the optimal process performance is the $K_{ext}/C_{NO_{x,max}}$ ratio. For the best performance, one must search for conditions that maximize this ratio. Figure 14 depicts the $K_{ext}/C_{NO_{x,max}}$ ratio as a function of X (reactor conversion) and R (recycle ratio). For X values in the range of 10−40%, increasing R decreases the $K_{ext}/C_{NO_{x,max}}$ ratio. On the other hand, when $X = 60-90\%$, increasing R and, therefore, the CO + CO_2 mole fraction in the fuel will increase $K_{ext}/C_{NO_{x,max}}$. Analysis indicates that, with a higher conversion, there is more CO produced, and this will result in a higher K_{ext} for the flame. However, high temperatures and NO_x emissions will also happen under these conditions, but under the condition of higher reactor conversions, the increase of K_{ext} will exceed the increase of NO_x, as the results of Figure 14 suggest.

Figure 15 correlates the process efficiency with $C_{NO_{x,max}}$ (for a given value of ϕ_{total}). Parameters on this figure are the reactor conversion, X, and the CO_2 recycle ratio, R. It is clear from this figure (and from the prior discussion) that increasing the reactor conversion noticeably increases the efficiency (and for the same reactor conversion so does increasing R). What is encouraging, however, is that for a range of reactor conversions this increase in the efficiency is also accompanied by a decrease in $C_{NO_{x,max}}$. When X reaches 60%, this is no longer true and the process efficiency and $C_{NO_{x,max}}$ follow the same increasing trend. This is

due to the increase of CO production, which results in a high temperature for these flames. Therefore, thermal NO_x production dominates, and the total NO_x concentration will increase as the efficiency increases.

Conclusions

A combined experimental and numerical investigation was conducted of a proposed advanced power generation cycle involving waste heat utilization through CO_2 decomposition using a high-temperature membrane reactor, which also produces pure O_2. This cycle may find application in the recovery of waste heat from high-temperature processes that utilize oxygen. Examples of such processes are the continuous recuperative furnaces employed in the glass industry. Because glass-making facilities have little use for utilities such as steam, the only option for recovering heat from the flue gas is air preheat. In the integrated process, the unused sensible heat of the furnace's flue gas is used to drive the dissociation of CO_2 to CO and O_2 in the membrane reactor. As a result, the waste heat in the flue gas is upgraded for use to either melt and fuse additional glass or reduce the fuel and oxygen requirements for a given process load. Extensive process design simulations indicate that the overall furnace efficiency is significantly increased.

To investigate further the feasibility of the proposed process, a number of $SrCo_{0.5}FeO_3$ membrane disks have been prepared and tested under both inert and reactive conditions. The O_2 permeabilities of these membranes under reactive conditions were shown to be significantly higher than those attained in inert environments. These membranes were tested in a membrane reactor for the decomposition of carbon dioxide. Conversions significantly higher than the corresponding equilibrium conversions were attained.

In this paper, aspects of flame stability and pollutant emissions for the overall process were also studied and presented. The requirements for maintaining good combustion stability and for minimizing pollutant emissions were analyzed for the wide variety of fuel compositions that may be employed in the cycle. A range of conditions appear to exist, for which the cycle allows for effective waste heat utilization without undue impact on pollutant emissions and combustion stability.

Acknowledgment

The support of the California Energy Commission through the Energy Innovations Small Grant (EISG) program is gratefully acknowledged.

Notation

C = concentration (ppm)
K = strain rate (s^{-1})
K_{ext} = extinction strain rate (s^{-1})
R = recycle ratio
X = membrane reactor conversion
Y = mole fraction

Sub- and Superscripts

max = maximum
stoich = stoichiometric

Greek Letter

ϕ = equivalence ratio

Literature Cited

(1) Ren, J. Y.; Tsotsis, T. T.; Egolfopoulos, F. N. Basic Aspects of Combustion Stability and Pollutant Emissions of a CO_2 Decomposition-Based Power-Generation Cycle. *Ind. Eng. Chem. Res.* **2002**, *41*, 4543.

(2) Ren, J. Y.; Qin, W.; Egolfopoulos, F. N.; Mak, H.; Tsotsis, T. T. Methane Reforming and its Potential Effect on the Efficiency and Pollutant Emissions of Lean Methane−Air Combustion. *Chem. Eng. Sci.* **2001**, *56*, 1541.

(3) Nigara, Y.; Cales, B. Production of CO by Direct Thermal Splitting of CO_2 at High Temperatures. *Bull. Chem. Soc. Jpn.* **1986**, *59*, 1997.

(4) Itoh, N.; Sanchez, M. A.; Xu, W.; Haraya, K.; Hongo, M. Application of Membrane Reactor System to Thermal Decomposition of CO_2. *J. Membr. Sci.* **1993**, *77*, 245.

(5) Frankie, B. M.; Zubrin, R. Chemical Engineering in Extraterrestrial Environments. *Chem. Eng. Prog.* **1999**, *95*, 45.

(6) Masri, A. R.; Dibble, R. W.; Barlow, R. S. Chemical Kinetic Effects in Non-Premixed Flame of H_2/CO_2 Fuel. *Combust. Flame* **1992**, *91*, 285.

(7) Qin, W.; Egolfopoulos, F. N.; Tsotsis, T. T. A Detailed Study of the Combustion Characteristics of Landfill Gas. *Chem. Eng. J.* **2001**, *3773*, 1.

(8) Balachandran, U.; Dusek, J. T.; Mieville, R. L.; Poeppel, R. B.; Kleefisch, M. S.; Pei, S.; Kobylinski, T. P.; Udovich, C. A.; Bose, A. C. Dense Ceramic Membranes for Partial Oxidation of Methane to Syngas. *Appl. Catal. A* **1995**, *133*, 19.

(9) Balachandran, U.; Ma, B.; Maiya, P. S.; Mieville, R. L.; Dusek, J. T.; Picciolo, J. J.; Guan, J.; Dorris, S. E.; Liu, M. Development of Mixed-conducting Oxides for Gas Separation. *Solid State Ionics* **1998**, *108*, 363.

(10) Lu, Y.; Dixon, A. G.; Moser, W. R.; Ma, Y. H.; Balachandran, U. Oxidative Coupling of Methane Using Oxygen-permeable Dense Membrane Reactors. *Catal. Today* **2000**, *56*, 297.

(11) Mitchell, B. J.; Richardson, J. W., Jr.; Murphy, C. D.; Ma, B.; Balachandran, U.; Hodges, J. P.; Jorgensen, J. D. Phase Stability of $SrFeCo_{0.5}O_y$ under Synthesis and Annealing Conditions. *J. Eur. Ceram. Soc.* **2002**, *22*, 661.

(12) Crane, R. G.; Hewitson, B. C. Double CO_2 Precipitation Changes for the Susquehanna Basin: Down-Scaling from the Genesis General Circulation Model. *Int. J. Climatol.* **1998**, *18*, 65.

(13) Betts, R. A.; Cox, P. M.; Woodward, F. I. Simulated Responses of Potential Vegetation to Double-CO_2 Climate Change and Feedbacks on Near-Surface Temperature. *Global Ecol. Biogeogr.* **2000**, *9*, 171.

(14) Egolfopoulos, F. N.; Campbell, C. S. Unsteady, Counterflowing, Strained Diffusion Flames: Frequency Response and Scaling. *J. Fluid Mech.* **1996**, *318*, 1.

(15) Law, C. K.; Egolfopoulos, F. N. A Unified Chani-Thermal Theory of Fundamental Flammability Limits. *Proc. Combust. Inst.* **1992**, *24*, 137.

(16) Egolfopoulos, F. N. Geometric and Radiation Effects on Steady and Unsteady Strained Laminar Flames. *Proc. Combust. Inst.* **1994**, *25*, 1375.

(17) Kee, R. J.; Rupley, F. M.; Miller, J. A. *Chemkin-II*: *A Fortran Chemical Kinetics Package for the Analysis of Gas-Phase Chemical Kinetics*; Report SAND89-8009; Sandia National Laboratories: Albuquerque, NM, 1989.

(18) Kee, R. J.; Warnatz, J.; Miller, J. A. *A Fortran Computer Code Package for the Evaluation of Gas-Phase Viscosities, Conductivities, and Diffusion Coefficients*; Report SAND83-8209; Sandia National Laboratories: Albuquerque, NM, 1983.

(19) Bowman, C. T.; Frenklach, M.; Gardiner, W. R.; Smith, G. The "GRI 3.0" Chemical Kinetic Mechanism, 1999; http://www.me.berkeley.edu/ gri_mech/.

(20) Boyd, D. C.; Danielson, P. S.; Thompson, D. A. *Kirk−Othmer Encyclopedia of Chemical Technology*; John Wiley & Sons: New York, 1994.

(21) Ren, J. Y.; Fan, Y.; Egolfopoulos, F. N.; Tsotsis, T. T. Membrane-Based Reactive Separations for Power Generation Applications: Oxygen Lancing. *Chem. Eng. Sci.* **2003**, *58*, 1043.

(22) Ren, J. Y.; Qin, W.; Egolfopoulos, F. N.; Tsotsis, T. T. Strain-Rate Effects on Hydrogen-Enhanced Lean Premixed Combustion. *Combust. Flame* **2001**, *124*, 717.

Received for review December 9, 2002
Revised manuscript received March 17, 2003
Accepted March 19, 2003

IE020980R